A&A 598, A100 (2017)
DOI: 10.1051/0004-6361/201629128

Astronomy & Astrophysics

Abundances of disk and bulge giants from high-resolution optical spectra

I. O, Mg, Ca, and Ti in the solar neighborhood and *Kepler* field samples[⋆,⋆⋆]

H. Jönsson[1,2,3], N. Ryde[1], T. Nordlander[4], A. Pehlivan Rhodin[1,5], H. Hartman[1,5], P. Jönsson[5], and K. Eriksson[4]

[1] Lund Observatory, Department of Astronomy and Theoretical Physics, Lund University, Box 43, 221 00 Lund, Sweden
e-mail: henrikj@astro.lu.se
[2] Instituto de Astrofísica de Canarias (IAC), 38205 La Laguna, Tenerife, Spain
[3] Universidad de La Laguna, Dpto. Astrofísica, 38206 La Laguna, Tenerife, Spain
[4] Department of Physics and Astronomy, Uppsala University, Box 516, 751 20 Uppsala, Sweden
[5] Materials Science and Applied Mathematics, Malmö University, 205 06 Malmö, Sweden

Received 16 June 2016 / Accepted 14 November 2016

ABSTRACT

Context. The Galactic bulge is an intriguing and significant part of our Galaxy, but it is hard to observe because it is both distant and covered by dust in the disk. Therefore, there are not many high-resolution optical spectra of bulge stars with large wavelength coverage, whose determined abundances can be compared with nearby, similarly analyzed stellar samples.
Aims. We aim to determine the diagnostically important alpha elements of a sample of bulge giants using high-resolution optical spectra with large wavelength coverage. The abundances found are compared to similarly derived abundances from similar spectra of similar stars in the local thin and thick disks. In this first paper we focus on the solar neighborhood reference sample.
Methods. We used spectral synthesis to derive the stellar parameters as well as the elemental abundances of both the local and bulge samples of giants. We took special care to benchmark our method of determining stellar parameters against independent measurements of effective temperatures from angular diameter measurements and surface gravities from asteroseismology.
Results. In this first paper we present the method used to determine the stellar parameters and elemental abundances, evaluate them, and present the results for our local disk sample of 291 giants.
Conclusions. When comparing our determined spectroscopic temperatures to those derived from angular diameter measurements, we reproduce these with a systematic difference of +10 K and a standard deviation of 53 K. The spectroscopic gravities reproduce those determined from asteroseismology with a systematic offset of +0.10 dex and a standard deviation of 0.12 dex. When it comes to the abundance trends, our sample of local disk giants closely follows trends found in other works analyzing solar neighborhood dwarfs, showing that the much brighter giant stars are as good abundance probes as the often used dwarfs.

Key words. solar neighborhood – Galaxy: evolution – stars: abundances

1. Introduction

How the Galactic bulge formed and evolved is an intriguing question that has been given a lot of attention in recent years (see for example Rich 2013; Gonzalez & Gadotti 2016; Di Matteo 2016, for reviews). There are three problems with observing the bulge: it is distant, so the stars are faint; it is obscured by the dust in the disk, so very little of the optical light emitted by the bulge stars reach us; and the crowding of stars makes it hard to place the slit of the spectrometer to avoid contaminating light from another star. For the first two problems it helps to observe luminous giant stars and, indeed, this has been the main method used; see for example Zoccali et al. (2006), Lecureur et al. (2007), Alves-Brito et al. (2010), González et al. (2011), Johnson et al. (2012, 2013, 2014).

One fact that could cause problems when analysing spectra from giant stars is the presence of molecules in their atmospheres. The molecules emerge since giant stars are generally cooler than the dwarf stars often used in spectroscopic investigations. A complication is therefore the increased number of lines, mainly due to rich molecular spectra. This might lead, particularly for the very coolest and most metal-rich stars, to the situation where the continuum close to the lines of interest cannot be identified even at very high spectral resolution. Since the abundance derived from a spectral line depends on the ratio of line to continuum opacities, large uncertainties are introduced if the continuum cannot be defined. A large density of lines might also form a psuedo-continuum, which could falsely be taken as a true continuum, thereby further complicating the analysis. The probability that spectral lines are blended, in the worst case by unknown lines or lines with uncertain line data, is increased by the presence of molecular lines. The spectral lines chosen for an abundance analysis should be as unblended as possible and not

⋆ Based on observations made with the Nordic Optical Telescope (programs 51-018 and 53-002), operated by the Nordic Optical Telescope Scientific Association at the Observatorio del Roque de los Muchachos, La Palma, Spain, of the Instituto de Astrofisica de Canarias, and on spectral data retrieved from PolarBase at Observatoire Midi Pyrénées.
⋆⋆ Full Tables A.1 and A.3 are only available at the CDS via anonymous ftp to cdsarc.u-strasbg.fr (130.79.128.5) or via http://cdsarc.u-strasbg.fr/viz-bin/qcat?J/A+A/598/A100

too deep and might therefore be rare in giants. As the problem worsens as the star is cooler, many works, including the bulge articles mentioned in the first paragraph (and this project), have restricted themselves to moderately cool K giants or red clump stars.

Furthermore, for sun-like stars, the abundance could be determined differentially by simply comparing the strength of the spectral line in question in the stellar spectrum to that of a solar spectrum. Such an approach for an analysis of giants is more complicated and might introduce large systematic uncertainties. If a solar spectrum is used in the comparison, in many cases unknown blending lines show up in the giant star spectra, leading to an overestimation of the abundance of the element in the giant star; if instead a spectrum of a giant star is used as a comparison, the zero point of the derived abundances are very uncertain because they rely on the accuracy of the abundances and stellar parameters of the comparison star and the completeness of the line list.

When giant stars are used in abundance works that investigate the bulge, for example, a good approach to deal with these problems is to make a strictly differential comparison between the abundances found in the bulge to those of the more known stellar population of the local disk. For example, Alves-Brito et al. (2010), found elemental abundances from their 25 bulge giants to be similar to those of the thick disk in their 55 similar giants from the solar neighborhood, and Bensby et al. (2013), using microlensed dwarfs, found that the "knee" in their [α/Fe] versus [Fe/H] plots likely was at slightly higher metallicities in their 58 bulge dwarfs as compared to their local disk sample of 714 stars (Bensby et al. 2014).

In this paper we present a compilation of a solar neighborhood sample of 291 local disk giants for which we determined the stellar parameters and abundances of the α elements oxygen, magnesium, calcium, and titanium. We demonstrate that we can determine the elemental abundances of giants with similar precision and accuracy as for dwarfs. In Paper II of this series (Jönsson et al. 2017), we use this solar neighborhood sample to compare differentially elemental abundances of giants in the bulge to abundances in the solar neighborhood. This is possible since we determine the stellar parameters and α abundances of the bulge sample in the same way.

The homogeneously analyzed local disk sample presented here might also be useful in other aspects. Since it includes stars in the *Kepler* field, the determined parameters might be used to revise the stellar properties for these stars (Huber et al. 2014) or the bright stars of the sample might be used as a basis for selecting and analyzing stars using smaller telescopes and/or less sensitive instruments, such as the mid-infrared spectrometer TEXES (Lacy et al. 2002). To our knowledge, the sample presented here is the largest spectroscopically analyzed sample of metal-rich giants using high-resolution optical spectra with large wavelength coverage.

2. Observations

2.1. The bulge sample

As mentioned in Sect. 1, the main purpose of this project is to analyze high-resolution optical spectra of bulge giants, but the analysis of the actual bulge spectra will be presented in Paper II of the series, while this paper concentrates on the analysis of a local disk comparison sample. The bulge sample consists of 46 K giants observed with FLAMES/UVES at VLT; the sample comprises 35 spectra that have been previously analyzed in Zoccali et al. (2006), Lecureur et al. (2007), Ryde et al. (2010), Barbuy et al. (2013), and Van der Swaelmen et al. (2016) and 11 spectra that have never been analyzed from a new bulge field even closer to the Galactic center with $(l, b) = (1.25, -2.65)$. More details on this sample will be given in Paper II.

2.2. The solar neighborhood sample

In this paper, Paper I in the series, we present the analysis of 291 giants in the solar neighborhood. We observed 150 of these giants via the spectrometer FIES (Telting et al. 2014) mounted on the Nordic Optical Telescope (NOT) under program 51-018 (May–June 2015) and 63 of these giants via FIES/NOT under program 53-002 (June 2016). We took 41 spectra from Thygesen et al. (2012) (in turn from FIES/NOT), and we downloaded 18 spectra from the FIES archive and 19 spectra from the NARVAL and ESPaDOnS spectral archive PolarBase (Petit et al. 2014).

The FIES spectra have $R \sim 67\,000$ and the PolarBase-spectra have $R \sim 65\,000$. They both cover the entire optical part of the spectrum, but only the region between 5800 Å and 6800 Å is used in the analysis, to be consistent with the analysis of the bulge spectra in Paper II.

Most of the stars observed are very bright and have typical observing times on the order of minutes. The 213 stars observed by us using FIES were observed using the `exp-count` feature, aborting the exposure when a specified CCD count level had been reached. Therefore, a vast majority of these spectra have a signal-to-noise ratio (S/N) of 80–120; see Table A.1. The spectra downloaded from PolarBase generally have similar S/N, the FIES-archive spectra generally have slightly higher S/N, while the spectra from Thygesen et al. (2012) have lower S/N of around 30–50. All S/N, as measured by the IDL-routine `der_snr.pro`[1], are listed in Table A.1.

Our FIES spectra were reduced using the standard FIES pipeline, while the spectra from Thygesen et al. (2012) and PolarBase were already reduced and ready to analyze. All spectra have been roughly normalized using the IRAF task `continuum`. In the analysis step a more careful continuum normalization is made for every wavelength window analyzed (see Sect. 3).

No sky subtraction and/or removal of telluric lines were attempted. Instead, regions of the spectra influenced by telluric absorption lines and bright sky emission lines were avoided; as can be seen in Fig. 1, telluric lines are affecting regions around the stellar oxygen and magnesium lines, while only the stellar oxygen line is affected by a possible sky emission line. The telluric lines and skyline affecting regions around the widely used 6300 Å oxygen line are important sources of uncertainties in the derived oxygen abundances in all works using this line.

The basic data for the analyzed disk giant stars are listed in Table A.1.

3. Analysis

The 291 local disk spectra analyzed in this paper and the 46 bulge spectra analyzed in Paper II were analyzed in the exact same way to ensure a strictly differential comparison.

We used the software `Spectroscopy Made Easy` (SME; Valenti & Piskunov 1996). The SME software simultaneously fits stellar parameters and/or abundances by fitting calculated synthetic spectra to an observed spectrum via χ^2 minimization. By selecting regions with spectral lines of interest and points

[1] See `http://www.stecf.org/software/ASTROsoft/DER_SNR`

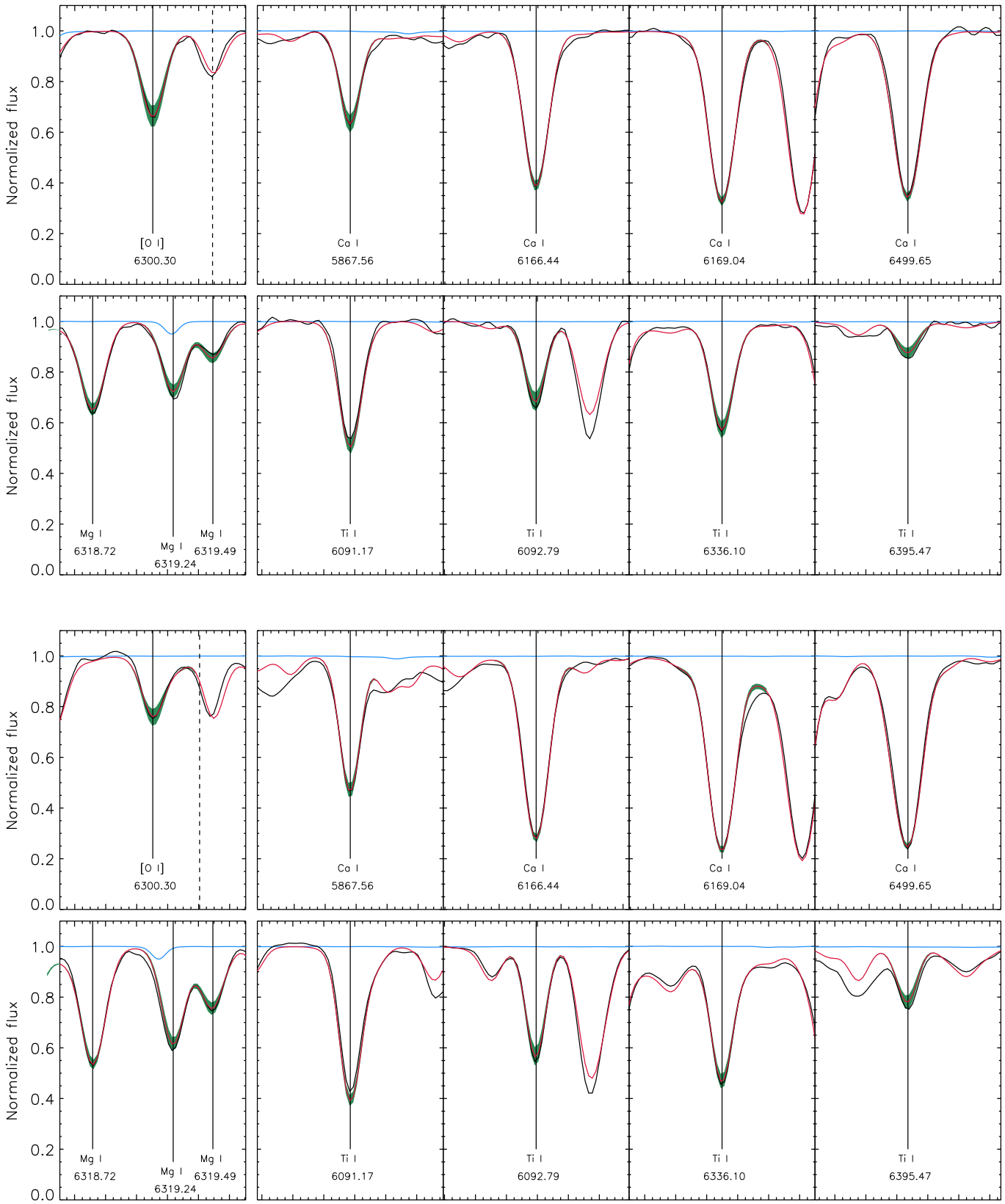

Fig. 1. Stellar lines used for abundance determinations in the analyzed FIES spectra of Arcturus and μLeo in *the top and bottom two rows*, respectively. The stellar spectrum is shown in black, the best-fitting synthetic spectrum in red, and ±0.1 dex of the element in question in green. The telluric spectrum from the Arcturus atlas of Hinkle et al. (2000) is shown in blue and the position of the bright 6300 Å sky emission line is shown with a dashed line. Stellar lines possibly affected by telluric absorption lines and/or sky emission lines were avoided in the analysis. All panels show 1.2 Å of spectra surrounding the line in question, i.e., the larger tickmarks indicate steps of 0.2 Å.

that SME should treat as continuum points, specific lines can be chosen as basis of the analysis. Special care was taken to avoid fitting spectral regions affected by telluric lines, which is particularly a problem for the oxygen and magnesium lines used.

In the analysis, we used LTE MARCS models that are spherical symmetric and [α/Fe] enhanced. Within the *Gaia*-ESO collaboration (Gilmore et al. 2012) SME has been modified to apply NLTE departure coefficients interpolated from the grid presented by Lind et al. (2012), which covers the stellar parameters and lines used in the analysis.

We determine all the stellar parameters ($T_{\rm eff}$, $\log g$, [Fe/H], and $\xi_{\rm micro}$) simultaneously, using relatively weak, unblended Fe I, Fe II, and Ca I lines and gravity-sensitive Ca I-wings (Edvardsson 1988). This means that the Ca abundance is fitted simultaneously as the stellar parameters, but all other abundances are determined with fixed stellar parameters. The atomic data of the spectral lines used are listed in Table A.2.

3.1. Line data

We took all the line data used, in both determining the stellar parameters and abundances, from version 5 of the *Gaia*-ESO line list (Heiter et al. 2015b) with some exceptions. We updated the wavelength data of all Fe II lines with values from Nave & Johansson (2013), and updated the $\log gf$ values from the calculated values of Raassen & Uylings (1998) to the astrophysical values of Meléndez & Barbuy (2009). The latter values produce better fitting synthetic spectra, and most importantly, produce spectroscopic surface gravities that are closer to the asteroseismic surface gravities for the *Kepler* stars in our sample. Furthermore, we updated the $\log gf$ values of the three Mg I lines used, from the calculated values of Butler et al. (1993) to values from Pehlivan Rhodin et al. (2017). There is an autoionizing Ca I line that is close to these Mg I lines, producing a very wide (up to 5 Å) and shallow depression in the spectra. We found that removing this line from the synthesis and, instead, placing a local continuum around the Mg I lines produced the tightest magnesium trend in our data. Therefore, we did not use any atomic data for the autoionizing Ca I line. Since we use the 6300.3083 Å [O I] line to determine oxygen abundance, the atomic data of the blending Ni I line at 6300.3419 Å is also of importance. Here we used the experimental $\log gf = -2.11$ from Johansson et al. (2003). In the analysis of the different stars, we used a solar Ni abundance scaled with the iron abundance of that particular star.

The line data of the lines used is listed in Table A.2. The final line list consists of 47 lines, of which 39 are used to determine the stellar parameters and the Ca abundance. All lines are situated in the wavelength range between 5800 Å to 6800 Å to match the usable range of the bulge spectra analyzed in Paper II, thereby enabling a strictly differential comparison.

Regarding the broadening of spectral lines due to collisions with neutral hydrogen (van der Waals broadening), the data for all the listed lines are taken from Barklem & Aspelund-Johansson (2005) and Barklem et al. (2000), with some exceptions not available in those references: for the Fe I line at 6793 Å, values from Kurucz (2007) are used; for the Ca I line at 5867 Å, values from Smith (1988) are used; for the 6300 Å [O I]-line, values from Wiese et al. (1966) are used, and for the three Mg I lines, values from Kurucz & Peytremann (1975) are used.

To minimize the errors and uncertainties in the determined stellar parameters and abundances we carefully checked all used lines for (known) blends in a grid of stellar atmospheres, following a similar method as in Jönsson et al. (2011). Typically a massive wealth of TiO molecular lines makes most lines in our wavelength range very hard to use for stars with temperatures below ~3900 K.

3.2. Random uncertainties in the stellar parameters

Random uncertainties in our method of determining the stellar parameters include both the freedom in setting the continuum and in the actual line fit. These obviously depend on the S/N of the observation in question. To test this, we degraded the Arcturus spectrum of Hinkle et al. (2000) to different S/N and determined the stellar parameters for those spectra. The IDL-routine `x_addnoise`[2] was used to inject noise and create 100 realizations each of Arcturus spectra with S/N of 10 to 120 in steps of 10. The parameters for these spectra were then derived exactly as for the science spectra, and the results are shown in the box plots in Fig. 2.

From Fig. 2 one can deduce that for a $S/N \gtrsim 50$ the uncertainties are on the same order, while they grow very large for $S/N \lesssim 20$, meaning that integration times, at least for Arcturus-like stars, preferably should be adjusted to reach a $S/N > 20$. But these integration times do not have to be so long that a much greater S/N than 50 is reached. However cooler and/or more metal-rich stars likely need higher S/N to resolve the more numerous lines, and also higher S/N is desired when determining abundances from a single line, which is the case for our oxygen abundances (see Table A.2). Of interest is also that mainly the "whiskers" of the plots expand for lower S/N, and the "boxes", holding 50% of the data, are more similarly sized as the S/N is lowered. This means that, even for the lowest S/N bins, we determine reasonable stellar parameters for a majority of the spectra.

Since all our program stars are bright, they have excellent S/N, in general around 100, and based on Fig. 2 we can therefore conclude that random uncertainties stemming from the quality of the spectrum for an Arcturus-like red giant would be very small, on the order $\delta T_{\rm eff} = \pm 10$ K, $\delta \log g = \pm 0.05$, δ[Fe/H] $= \pm 0.02$, $\delta v_{\rm mic} = \pm 0.02$ (standard deviation). Instead our uncertainties are dominated by the systematic uncertainties evaluated in the next section.

In Paper II, the uncertainties of the stellar parameters and abundances derived from the observations of the very faint bulge stars will in many cases be dominated by random uncertainties stemming from the S/N.

3.3. Systematic uncertainties in the stellar parameters

Systematic uncertainties in stellar parameters and abundances are very hard to assess. They stem from everything from uncertainties in the atomic data used to simplifications in the stellar atmosphere models. To assess these systematic uncertainties of the stellar parameters, we evaluate them in three steps by comparison with trusted benchmark values.

Firstly, we compare our derived stellar parameters to those three overlapping with the *Gaia* benchmark stars (Heiter et al. 2015a; Jofré et al. 2014, 2015). Our results and the benchmark values are listed in Table 1. For these three stars, we find our parameters to be within the uncertainties of the benchmark values with one exception: our $\log g$ for μLeo is slightly higher. In general all our surface gravities are slightly higher than the three

[2] `http://www.ucolick.org/~xavier/IDL/`

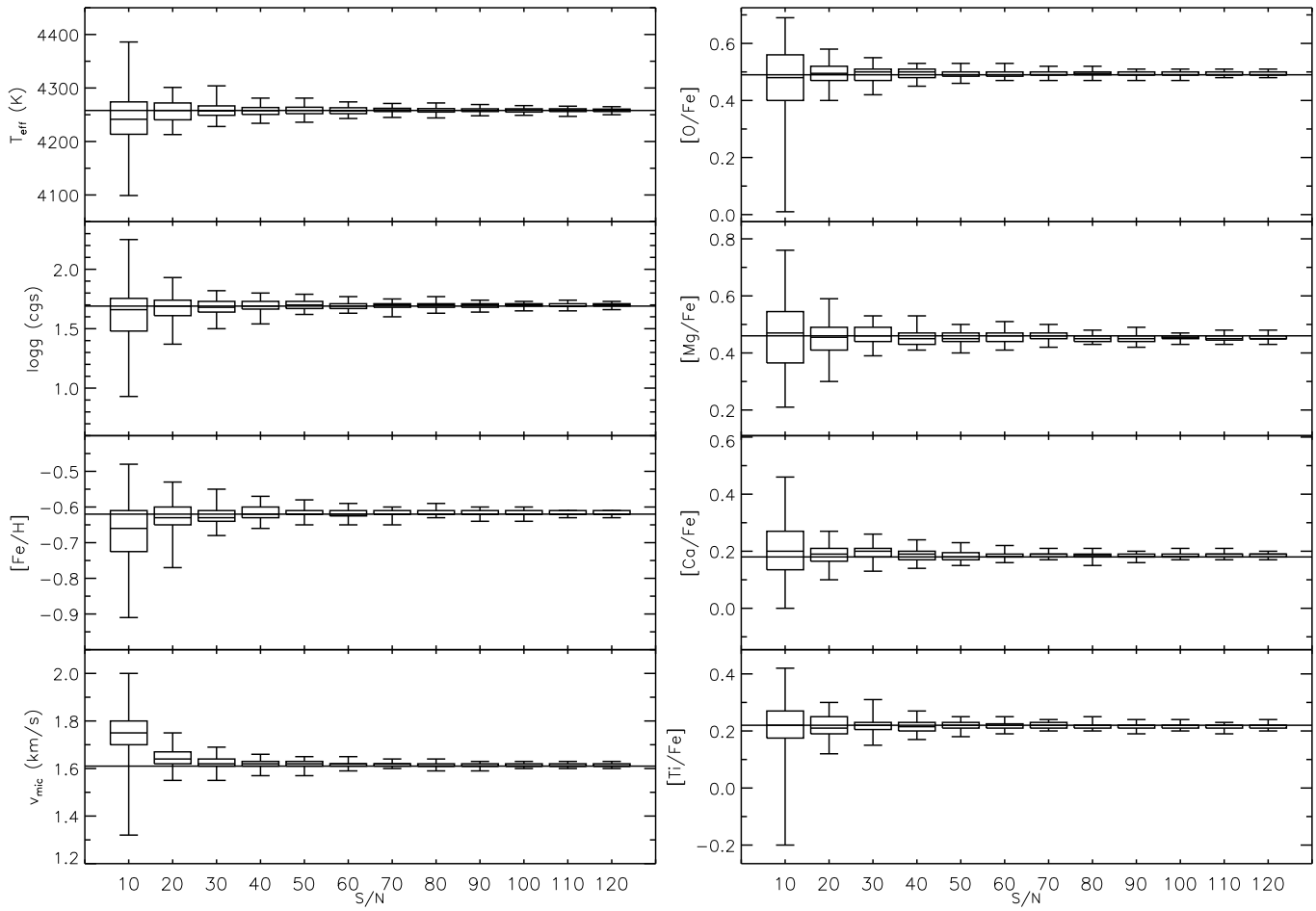

Fig. 2. Results from determining the stellar parameters and abundances for Arcturus spectra with different injected S/N. The horizontal line crossing each panel represents the value as determined from the original, high-S/N, atlas spectrum. The horizontal line in the boxes shows the median of the data, the lower and upper boundaries of the boxes show the lower and upper quartiles of the data, and the whiskers extend to the lowest and highest value of the data.

Table 1. *Gaia* stellar parameter benchmark values (Heiter et al. 2015a; Jofré et al. 2014, 2015) listed for the three giants in our sample.

HIP	Name	$T_{\rm eff}$	log g	[Fe/H]	$v_{\rm mic}$	A(O)	A(Mg)	A(Ca)	A(Ti)
HIP 37826	β Gem	4858 ± 60	2.90 ± 0.08	0.08 ± 0.16	1.28 ± 0.21	...	7.56 ± 0.07	6.40 ± 0.08	4.96 ± 0.07
		4835	2.93	0.04	1.24	8.69	7.63	6.43	4.92
HIP 48455	μ Leo	4474 ± 60	2.51 ± 0.11	0.20 ± 0.15	1.28 ± 0.26	...	8.11 ± 0.11	6.60 ± 0.12	5.22 ± 0.10
		4461	2.65	0.20	1.55	8.93	7.83	6.50	5.13
HIP 69673	αBoo	4286 ± 35	1.64 ± 0.09	−0.57 ± 0.08	1.58 ± 0.12	...	7.49 ± 0.09	5.92 ± 0.13	4.59 ± 0.08
		4251	1.72	−0.60	1.64	8.57	7.38	5.88	4.54
		4258	1.69	−0.62	1.61	8.56	7.44	5.91	4.55

Notes. The stellar values determined using our analysis for the corresponding star are listed below. In the case of Arcturus (HIP 68673), we have two determinations: the first row shows our results using our FIES-spectrum, and the second row shows our results using the atlas of Hinkle et al. (2000). [Fe/H] is listed in the Asplund et al. (2009) scale, i.e., with $A(\rm Fe)_\odot$ = 7.50.

benchmark values, but for the other two stars our results are as stated within the uncertainties.

Secondly, except for Arcturus, β Gem, and μ Leo, nine of our program stars have temperatures determined from angular diameter measurements (Mozurkewich et al. 2003); see Table 2. Our determined temperatures are within the uncertainties from the temperatures of Mozurkewich et al. (2003) with one exception: β UMi, for which we derive a temperature that is 143 K higher than the reference value, showing the difficulty in determining the temperatures for the very coolest stars. All in all, we are able to derive the temperatures of these stars with a systematic offset of +10 K and a standard deviation of 53 K, which is very similar to the mean of the uncertainties of the measurements of Mozurkewich et al. (2003), i.e., 56 K.

Thirdly, when it comes to the surface gravity, our sample includes 39 giants in the *Kepler* field with asteroseismic gravities (Thygesen et al. 2012; Huber et al. 2014); our determined gravities deviate from the seismic values with a systematic offset of +0.10 dex and a standard deviation of 0.12 dex.

Table 2. Effective temperatures as derived based on angular diameter measurements (Mozurkewich et al. 2003) listed for the nine giants in our sample.

HIP	Name	$T_{\rm eff,ref}$	$T_{\rm eff}$	$\log g$	[Fe/H]
HIP 9884	α Ari	4493 ± 55	4464	2.27	–0.24
HIP 46390	α Hya	4060 ± 50	4095	1.56	–0.10
HIP 54539	ψ UMa	4550 ± 56	4534	2.33	–0.10
HIP 55219	ν UMa	4091 ± 50	4133	1.65	–0.17
HIP 72607	β UMi	3849 ± 47	3992	1.32	–0.23
HIP 74666	δ Boo	4850 ± 60	4861	2.63	–0.37
HIP 77070	α Ser	4558 ± 56	4540	2.61	0.16
HIP 94376	δ Dra	4851 ± 67	4807	2.71	–0.17
HIP 102488	ϵ Cyg	4756 ± 59	4711	2.59	–0.18

Notes. Also listed are the stellar parameters determined using our analysis based on observations from a FIES, NARVAL, or ESpaDOnS spectrum for the corresponding star.

Table 3. Uncertainties of the derived abundances of a typical star (our FIES Arcturus spectrum) for changes in the derived stellar parameters.

Uncertainty	δA(O)	δA(Mg)	δA(Ti)
$\delta T_{\rm eff}$ = −50 K	−0.01	+0.01	−0.07
$\delta T_{\rm eff}$ = +50 K	+0.01	±0.00	+0.07
$\delta \log g$ = −0.15	−0.07	−0.02	−0.01
$\delta \log g$ = +0.15	+0.06	+0.03	+0.01
δ[Fe/H]= −0.05	+0.02	±0.00	±0.00
δ[Fe/H]= +0.05	−0.01	±0.00	±0.00
$\delta v_{\rm mic}$ = −0.1	±0.00	0.01	+0.02
$\delta v_{\rm mic}$ = +0.1	−0.01	−0.01	−0.02

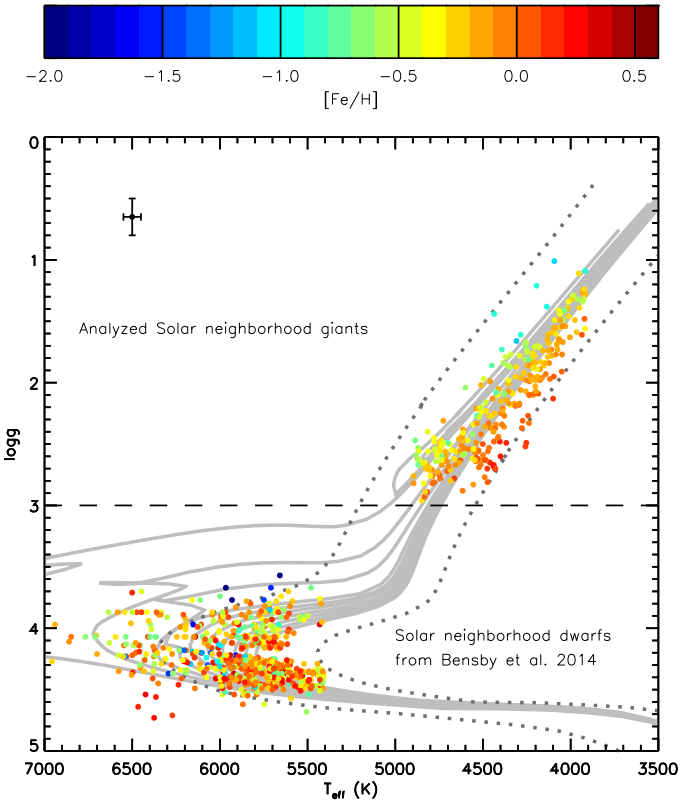

Fig. 3. HR diagrams for the observed giants and the 604 solar neighborhood dwarfs of Bensby et al. (2014) with $T_{\rm eff}$ > 5400 K. As a guide for the eye, isochrones with [Fe/H] = 0.0 and ages 1–10 Gyr are plotted using solid light gray lines. Furthermore, one isochrone with [Fe/H] = −1.0 and age 10 Gyr, and one with [Fe/H] = +0.5 and age 10 Gyr are plotted using dotted dark gray lines (Bressan et al. 2012). The parameters of the analyzed giants are determined from spectroscopy as described in the text. They line up as expected from isochrones in both temperature and surface gravity as well as metallicity. Expected, typical uncertanties are denoted in the top left corner of the plot.

To conclude, our determined effective temperatures seem very precise with a systematic shift of only +10 K, while we likely have a systematic shift of +0.1 dex in surface gravity. Regarding the metallicity, we only have three benchmark values, but our results are accurate with respect to those values.

3.4. Uncertainties in the determined abundances

When it comes to the uncertainties in the determined abundances, we assess and estimate them below in three steps.

Firstly, in the rightmost panels of Fig. 2, we show the determined abundances in the S/N-injected spectra, using the stellar parameters as determined in the same S/N-injected spectrum (those that are shown in the leftmost panels). As expected, the uncertainties in the determined abundances follow the uncertainties in the stellar parameters and show very large uncertainties for the lowest S/N bin. However, as for the stellar parameters, the box holding 50% of the values is still reasonably small, meaning that we still derive acceptable abundances for a majority of the spectra. Based on this investigation, the influence of S/N of the determined abundances of the high-S/N stars in this paper, is negligible, but it might be significant for some of the bulge spectra of Paper II having $S/N < 20$.

Secondly, in addition to the stellar parameters, Table 1 also lists the abundances of the three stars overlapping between Heiter et al. (2015a), Jofré et al. (2014, 2015) and our sample. Our abundances fall within the uncertainties of the benchmark values with one obvious and one more subtle exception. Firstly, our derived magnesium abundance of μLeo is much lower than the value from Jofré et al. (2015). We cannot find any reason for this discrepancy, but the benchmark value would place μLeo significantly above the [Mg/Fe] versus [Fe/H] trend shown in Fig. 4 at ([Fe/H]; [Mg/Fe]) = (0.20; 0.31), while our result follows the rest of the disk stars with ([Fe/H]; [Mg/Fe]) = (0.20; 0.03). Secondly, our magnesium abundance as derived from the FIES spectrum of Arcturus is also slightly lower than the benchmark value including its uncertainty. The abundance as derived from the Hinkle et al. (2000) atlas spectrum, however, is within the uncertainties of the benchmark value. The magnesium abundances, as derived from the FIES spectrum and the atlas spectrum, are deviating more than the abundances of oxygen, calcium, and titanium. Since the magnesium lines, as described in Sect. 3.1, have a neighboring autoionizing line whose curving influence on the continuum is hard to get rid of, it is not unexpected for the magnesium abundance of these high-S/N spectra to show higher uncertainty than the other abundances.

Thirdly, the uncertainties of determined abundances are often dominated by the uncertainties of the stellar parameters, and as is suggested by the similar shapes of the parameter boxes and the abundance boxes in Fig. 2, this is likely the case in this study. To estimate these uncertainties, often a table such as Table 3 is used. This table is best used as a way of telling which abundances are most uncertain and which parameter is mainly influencing the different abundances. For example, our probable systematic error of +0.1 dex in determining the $\log g$ mainly

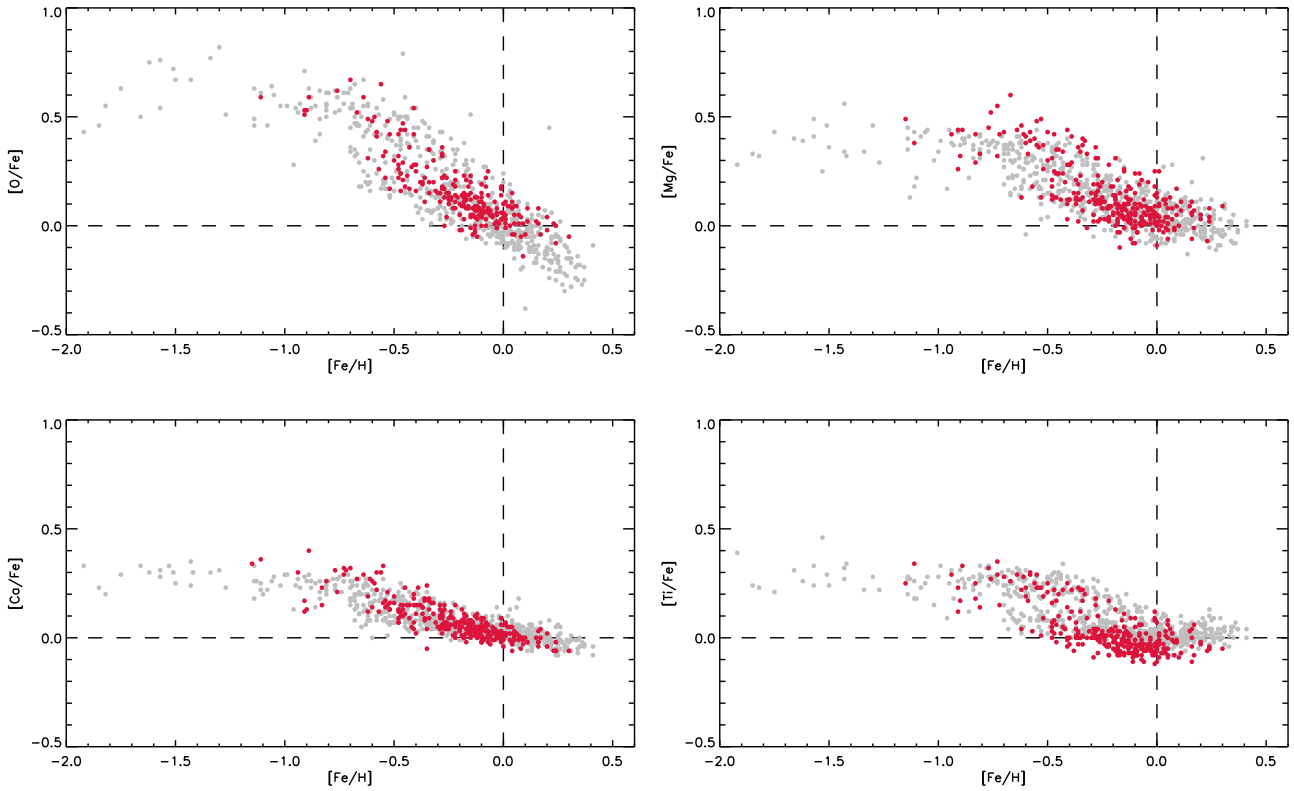

Fig. 4. [X/Fe] for the observed giants in red, compared to abundances of the 604 solar neighborhood dwarf stars of Bensby et al. (2014) with $T_{\rm eff}$ > 5400 K in gray. Especially for O and Ti a clear separation of thin and thick disk-type abundances can be seen in our sample. Since our sample is mostly made up of the very brightest, closest, giants, it is not surprising that a majority of the stars show thin disk-type chemistry. In the plots we use $A(\rm O)_\odot$ = 8.69, $A(\rm Mg)_\odot$ = 7.60, $A(\rm Ca)_\odot$ = 6.34, $A(\rm Ti)_\odot$ = 4.95, and $A(\rm Fe)_\odot$ = 7.50 (Asplund et al. 2009).

influences the oxygen abundance, while the titanium abundance is not affected by this systematic error. Estimating the total uncertainty in the abundance determination by adding the different uncertainties in quadrature would overestimate the uncertainties, since the parameters are coupled and deriving an incorrect temperature would possibly lead to an incorrect metallicity, for example. Furthermore, such an exercise would be based on the uncertainties of the stellar parameters, which in themselves are hard to estimate (compare Sect. 3.2).

To conclude, we can estimate expected typical uncertainties of the determined abundances to be almost on the order of 0.1 dex for magnesium and likely lower for the other abundances.

4. Results

The HR diagram, based on the spectroscopically determined stellar parameters of the observed giants, are shown in Fig. 3. Also the 604 solar neighborhood dwarf stars of Bensby et al. (2014), with $T_{\rm eff}$ > 5400 K and a collection of isochrones (Bressan et al. 2012), are shown in Fig. 3.

Our derived abundances for the giants can be seen in Table A.3 and Fig. 4. As a comparison, the corresponding abundances as derived in a local disk sample of dwarf stars by Bensby et al. (2014) are also shown in the figure.

5. Discussion

The aim of this analysis is twofold: to find as accurate stellar parameters and abundances as possible from giants, but most importantly, to collect a sample of homogeneously analyzed solar neighborhood targets similar to the bulge targets that will be presented in Paper II. The second aim means that we have to restrict our present analysis to the wavelength coverage of the bulge spectra even if the spectra analyzed here have wider coverage. In turn, this optional restriction might lead to a possibly lower precision of the abundances in the solar neighborhood sample that what would have been possible to attain using the entire coverage available from FIES, NARVAL, and ESpaDOnS.

The low deviations of the temperatures and gravities determined when compared to the more accurate angular diameter and asteroseismic measurements, together with the alignment in of the measurements along the red giant branch and spread in [Fe/H] in the HR diagram (Fig. 3), give us assurance that the method used is likely finding accurate values for the stellar parameters.

Estimating the formal uncertainties in abundance determinations is difficult. In our case, where we have very high S/N spectra and we are only using spectral lines with precise atomic data that are believed to be unblended, the main uncertainty of the abundances comes from the uncertainties of the stellar parameters. As elaborated in Sect. 3.4, the often used approach of adding the dependencies of the abundances on individual stellar parameters (Table 3) gives an overestimation on the total abundance uncertainty. All in all, our results show very similar trends as the carefully analyzed dwarfs in Bensby et al. (2014) in Fig. 4 and also have similarly tight trends, which hints at high precision in our derived abundances. The mean of the uncertainties quoted in Bensby et al. (2014) for the 604 stars with $T_{\rm eff}$ > 5400 K are δA(O) ∼ 0.14, δA(Mg) ∼ 0.06, δA(Ca) ∼ 0.06, δA(Ti) ∼ 0.07, and our uncertainties are thus likely at the same order. In the case of magnesium our scatter

is higher, hinting at a larger uncertainty, but in the case of oxygen our trend looks tighter, hinting at a lower mean uncertainty than that of Bensby et al. (2014). This is not unexpected since Bensby et al. use the very NLTE-sensitive oxygen triplet around 7771–7775 Å (Amarsi et al. 2016), although with corrections, making their oxygen abundances less precise than their other abundances; this fact is reflected in their higher quoted uncertainty for oxygen as mentioned above.

Based on the comparison between our abundance trends using K giants and those of the carefully analyzed dwarfs of Bensby et al. (2014), we would like to claim that giant stars are as good abundance indicators as dwarfs. This is an important point since the intrinsically brighter giants can be seen at much larger distances. As described in Sect. 1, however, care must be shown to possible blending lines, continuum fitting, and the atomic and/or molecular data for the used spectral lines.

6. Conclusions

The main purpose of this paper is to analyze a sample of local disk K giants to be used as a comparison sample for the similar sample of bulge giants to be analyzed in Paper II. To be certain that the local sample can be differentially compared to the stars in the bulge, where photometry is difficult and uncertain, we chose a strictly spectroscopic approach. Furthermore, we chose to restrict our analysis to the useful part of the bulge spectra, i.e., 5800–6800 Å. When we compare the determined effective temperatures to those derived from angular diameter measurements, we reproduce these with a systematic difference of +10 K and a standard deviation of 53 K. The spectroscopic gravities reproduce those determined from asteroseismology with a systematic offset of +0.10 dex and a standard deviation of 0.12 dex. Regarding the abundance trends, our sample of local disk giants closely follows that of the solar neighborhood dwarfs of Bensby et al. (2014) with similar spread and no obvious systematic differences.

Ideally, our sample should have consisted of more stars with typical thick disk abundances to better represent both local disk stellar populations, and we plan to expand the sample accordingly in the near future.

Acknowledgements. We thank Anders Thygesen and his collaborators for offering the reduced spectra of their stars online, and for kindly providing the observation dates and times to enable a scan for telluric contamination. We thank John Telting for help with the FIES data and, in particular, archive data. This research has been partly supported by the Lars Hierta Memorial Foundation, and the Royal Physiographic Society in Lund through Stiftelsen Walter Gyllenbergs fond and Märta och Erik Holmbergs donation. H.H., P.J., and N.R. acknowledges support from the Swedish Research Council, VR (project numbers 2011-4206, 2014-5640, and 2015-4842). This publication made use of the SIMBAD database, operated at CDS, Strasbourg, France, NASA's Astrophysics Data System, and the VALD database, operated at Uppsala University, the Institute of Astronomy RAS in Moscow, and the University of Vienna.

References

Aldenius, M., Lundberg, H., & Blackwell-Whitehead, R. 2009, A&A, 502, 989
Alves-Brito, A., Meléndez, J., Asplund, M., Ramírez, I., & Yong, D. 2010, A&A, 513, A35
Amarsi, A. M., Asplund, M., Collet, R., & Leenaarts, J. 2016, MNRAS, 455, 3735
Asplund, M., Grevesse, N., Sauval, A. J., & Scott, P. 2009, ARA&A, 47, 481
Barbuy, B., Hill, V., Zoccali, M., et al. 2013, A&A, 559, A5
Bard, A., & Kock, M. 1994, A&A, 282, 1014 (BK)
Bard, A., Kock, A., & Kock, M. 1991, A&A, 248, 315 (BKK)
Barklem, P. S., & Aspelund-Johansson, J. 2005, A&A, 435, 373 (BA-J)
Barklem, P. S., Piskunov, N., & O'Mara, B. J. 2000, A&AS, 142, 467 (BPM)
Bensby, T., Yee, J. C., Feltzing, S., et al. 2013, A&A, 549, A147
Bensby, T., Feltzing, S., & Oey, M. S. 2014, A&A, 562, A71
Blackwell, D. E., Petford, A. D., Shallis, M. J., & Simmons, G. J. 1982a, MNRAS, 199, 43
Blackwell, D. E., Petford, A. D., & Simmons, G. J. 1982b, MNRAS, 201, 595
Blackwell, D. E., Booth, A. J., Menon, S. L. R., & Petford, A. D. 1986, MNRAS, 220, 289
Bressan, A., Marigo, P., Girardi, L., et al. 2012, MNRAS, 427, 127
Butler, K., Mendoza, C., & Zeippen, C. J. 1993, J. Phys. B At., 26, 4409
Den Hartog, E. A., Ruffoni, M. P., Lawler, J. E., et al. 2014, ApJS, 215, 23
Di Matteo, P. 2016, PASA, 33, 027
Edvardsson, B. 1988, A&A, 190, 148
Froese Fischer, C., & Tachiev, G. 2012, Multiconfiguration Hartree-Fock and Multiconfiguration Dirac-Hartree-Fock Collection, Version 2, available online at http://physics.nist.gov/mchf/
Fuhr, J. R., Martin, G. A., & Wiese, W. L. 1988, J. Phys. Chem. Ref. Data 17 (New York: AIP and American Chemical Society) (FMW)
Gilmore, G., Randich, S., Asplund, M., et al. 2012, The Messenger, 147, 25
Gonzalez, O. A., & Gadotti, D. A. 2016, Galactic Bulges (Springer International Publishing Switzerland), Astrophys. Space Sci. Lib., 418, 199
González, O. A., Rejkuba, M., Zoccali, M., et al. 2011, A&A, 530, A54
Heiter, U., Jofré, P., Gustafsson, B., et al. 2015a, A&A, 582, A49
Heiter, U., Lind, K., Asplund, M., et al. 2015b, Phys. Scrip., 90, 054010
Hinkle, K., Wallace, L., Valenti, J., & Harmer, D. 2000, Visible and Near Infrared Atlas of the Arcturus Spectrum 3727–9300 A (ASP Monograph Publ.)
Huber, D., Silva Aguirre, V., Matthews, J. M., et al. 2014, ApJS, 211, 2
Jofré, P., Heiter, U., Soubiran, C., et al. 2014, A&A, 564, A133
Jofré, P., Heiter, U., Soubiran, C., et al. 2015, A&A, 582, A81
Johansson, S., Litzén, U., Lundberg, H., & Zhang, Z. 2003, ApJ, 584, L107
Johnson, C. I., Rich, R. M., Kobayashi, C., & Fulbright, J. P. 2012, ApJ, 749, 175
Johnson, C. I., McWilliam, A., & Rich, R. M. 2013, ApJ, 775, L27
Johnson, C. I., Rich, R. M., Kobayashi, C., Kunder, A., & Koch, A. 2014, AJ, 148, 67
Jönsson, H., Ryde, N., Nissen, P. E., et al. 2011, A&A, 530, A144
Jönsson, H., Ryde, N., Schultheis, M., & Zoccali, M. 2017, A&A, 598, A101 (Paper II)
Kurucz, R. L. 2007, Robert L. Kurucz on-line database of observed and predicted atomic transitions [arXiv:0704.2860]
Kurucz, R. L. 2013, Robert L. Kurucz on-line database of observed and predicted atomic transitions, Astrophys. Source Code Libr. [record ascl:1303.024]
Kurucz, R. L., & Peytremann, E. 1975, SAO Spec. Rep., 362, 1 (KP)
Lacy, J. H., Richter, M. J., Greathouse, T. K., Jaffe, D. T., & Zhu, Q. 2002, PASP, 114, 153
Lawler, J. E., Guzman, A., Wood, M. P., Sneden, C., & Cowan, J. J. 2013, ApJS, 205, 11
Lecureur, A., Hill, V., Zoccali, M., et al. 2007, A&A, 465, 799
Lind, K., Bergemann, M., & Asplund, M. 2012, MNRAS, 427, 50
May, M., Richter, J., & Wichelmann, J. 1974, A&AS, 18, 405 (MRW)
Meléndez, J., & Barbuy, B. 2009, A&A, 497, 611
Mozurkewich, D., Armstrong, J. T., Hindsley, R. B., et al. 2003, AJ, 126, 2502
Nave, G., & Johansson, S. 2013, ApJS, 204, 1
O'Brian, T. R., Wickliffe, M. E., Lawler, J. E., Whaling, W., & Brault, J. W. 1991, J. Opt. Soc. Am. B Opt. Phys., 8, 1185 (BWL)
Pehlivan Rhodin, A., Hartman, H., Nilsson, H., & Jönsson, P. 2017, A&A, 598, A102
Petit, P., Louge, T., Théado, S., et al. 2014, PASP, 126, 469
Raassen, A. J. J., & Uylings, P. H. M. 1998, A&A, 340, 300 (RU)
Ralchenko, Y., Kramida, A., Reader, J., & NIST ASD Team 2010, NIST Atomic Spectra Database (ver. 4.0.0), [Online]
Rich, R. M. 2013, in Planets, Stars and Stellar System, Vol. 5 (Springer), eds. T. D. Oswalt, & G. Glimore, 271
Ruffoni, M. P., Den Hartog, E. A., Lawler, J. E., et al. 2014, MNRAS, 441, 3127
Ryde, N., Gustafsson, B., Edvardsson, B., et al. 2010, A&A, 509, 20
Smith, G. 1981, A&A, 103, 351 (Sm)
Smith, G. 1988, J. Phys. B At. Mol. Phys., 21, 2827 (S)
Smith, G., & O'Neill, J. A. 1975, A&A, 38, 1 (SN)
Smith, G., & Raggett, D. S. J. 1981, J. Phys. B At. Mol. Phys., 14, 4015 (SR)
Storey, P. J., & Zeippen, C. J. 2000, MNRAS, 312, 813
Telting, J. H., Avila, G., Buchhave, L., et al. 2014, Astron. Nachr., 335, 41
Thygesen, A. O., Frandsen, S., Bruntt, H., et al. 2012, A&A, 543, A160
Valenti, J. A., & Piskunov, N. 1996, A&AS, 118, 595
Van der Swaelmen, M., Barbuy, B., Hill, V., et al. 2016, A&A, 586, A1
Wiese, W. L., Smith, M. W., & Glennon, B. M. 1966, Atomic transition probabilities, Vol.: Hydrogen through Neon. A critical data compilation (US Government Printing Office) (WSG)
Zoccali, M., Lecureur, A., Barbuy, B., et al. 2006, A&A, 457, L1

Appendix A: Additional tables

Table A.1. Basic data for the observed giants.

HIP/KIC/TYC	Alternative name	RA (J2000) (h:m:s)	Dec (J2000) (d:am:as)	V	$v_{\rm rad}$ km s^{-1}	S/N	Source
HIP 1692	H D1690	00:21:13.32713	–08:16:52.1625	9.18	18.37	114	FIES-archive
HIP 9884	alfAri	02:07:10.40570	+23:27:44.7032	2.01	–14.29	90	PolarBase
HIP 10085	HD 13189	02:09:40.17260	+32:18:59.1649	7.56	26.21	156	FIES-archive
HIP 12247	81Cet	02:37:41.80105	–03:23:46.2201	5.66	9.34	176	FIES-archive
HIP 28417	HD 40460	06:00:06.03883	+27:16:19.8614	6.62	100.64	121	PolarBase
HIP 33827	HR2581	07:01:21.41827	+70:48:29.8674	5.69	–17.99	79	PolarBase
HIP 35759	HD5 7470	07:22:33.85798	+29:49:27.6626	7.67	–30.19	85	PolarBase
HIP 37447	alfMon	07:41:14.83257	–09:33:04.0711	3.93	11.83	71	Thygesen et al. (2012)
HIP 37826	betGem	07:45:18.94987	+28:01:34.3160	1.14	3.83	90	PolarBase
HIP 43813	zetHya	08:55:23.62614	+05:56:44.0354	3.10	23.37	147	PolarBase

Notes. Coordinates and magnitudes are taken from the SIMBAD database, while the radial velocities are measured from the spectra. The S/N per data point is measured by the IDL-routine `der_snr.pro`, see http://www.stecf.org/software/ASTROsoft/DER_SNR. This is only an excerpt of the table to show its form and content. The complete table is available in electronic form at the CDS.

Table A.2. Atomic data for the spectral lines used in the analysis.

Element	Wavelength (Å) (air)	$\log gf$	$\chi_{\rm exc}$ (eV)	References
Fe I	5778.4533	–3.430	2.588	1, 2, 1
Fe I	5855.0758	–1.478	4.608	1, 2, 1
Fe I	6012.2098	–4.038	2.223	1, 3, 1
Fe I	6027.0508	–1.089	4.076	1, 4, 1
Fe I	6120.2464	–5.970	0.915	1, 5, 1
Fe I	6136.9938	–2.950	2.198	1, 4+6, 1
Fe I	6151.6173	–3.295	2.176	1, 3+4+6, 1
Fe I	6165.3598	–1.473	4.143	1, 4, 1
Fe I	6173.3343	–2.880	2.223	1, 6, 1
Fe I	6213.4294	–2.481	2.223	1, 4, 1
Fe I	6271.2779	–2.703	3.332	1, 2, 1
Fe I	6322.6850	–2.430	2.588	1, 4+7, 1
Fe I	6335.3299	–2.177	2.198	1, 4, 1
Fe I	6411.6480	–0.596	3.654	1, 3+4+8, 1
Fe I	6518.3657	–2.438	2.832	1, 2+4, 1
Fe I	6581.2092	–4.679	1.485	1, 3, 1
Fe I	6593.8695	–2.420	2.433	1, 4+6, 1
Fe I	6609.1097	–2.691	2.559	1, 4+7, 1
Fe I	6633.7487	–0.799	4.559	1, 4, 1
Fe I	6739.5204	–4.794	1.557	1, 3, 1
Fe I	6793.2582	–2.326	4.076	1, 2, 1
Fe I	6810.2622	–0.986	4.607	1, 4, 1
Fe I	6828.5912	–0.820	4.638	9, 10, 1
Fe I	6837.0056	–1.687	4.593	1, 2, 1
Fe I	6843.6554	–0.730	4.549	1, 11, 1
Fe II	5991.3721	–3.540	3.153	12, 13, 14
Fe II	6084.1030	–3.790	3.200	12, 13, 14
Fe II	6113.3192	–4.140	3.221	12, 13, 14
Fe II	6149.2459	–2.690	3.889	12, 13, 14
Fe II	6247.5590	–2.300	3.892	12, 13, 14
Fe II	6432.6772	–3.570	2.891	12, 13, 14
Fe II	6456.3805	–2.050	3.903	12, 13, 14
Ca I	5867.5620	–1.570	2.933	15, 15, 15
Ca I*	6122.2170	–0.380	1.886	16, 17, 16
Ca I*	6162.1730	–0.170	1.899	16, 17, 16
Ca I	6166.4390	–1.142	2.521	18+19, 18, 18+19
Ca I	6169.0420	–0.797	2.523	18+19, 18, 18+19
Ca I*	6439.0750	0.390	2.526	18+19, 18, 18+19
Ca I	6499.6500	–0.818	2.523	18+19, 18, 18+19
O I	6300.3038	–9.715	0.000	20, 21+22, 23
Mg I	6318.7170	–2.020	5.108	23, 24, 23
Mg I	6319.2370	–2.242	5.108	23, 24, 23
Mg I	6319.4930	–2.719	5.108	23, 24, 23
Ti I	6091.1710	–0.320	2.267	25, 26, 25
Ti I	6092.7918	–1.380	1.887	25, 26, 25
Ti I	6336.0993	–1.690	1.443	25, 26, 25
Ti I	6395.4718	–2.540	1.503	25, 26, 25

Notes. The first part list the lines used in the determination of the stellar parameters and calcium abundance, while the second part list the lines used to determine the oxygen, magnesium, and titanium abundances. All atomic data are collected by the *Gaia*-ESO line list group (Heiter et al. 2015b). For the three Ca I-lines denoted with asterisks only the gravity-sensitive wings are used. The references are for wavelength, $\log gf$, and excitation energy, respectively. In cases where several references are given for a quantity, the value listed is a mean of the reference values.

References. (1) Kurucz (2007); (2) Bard & Kock (1994); (3) Bard et al. (1991); (4) O'Brian et al. (1991); (5) Blackwell et al. (1986); (6) Blackwell et al. (1982a); (7) Blackwell et al. (1982b); (8) Den Hartog et al. (2014); (9) Fuhr et al. (1988); (10) May et al. (1974); (11) Ruffoni et al. (2014); (12) Nave & Johansson (2013); (13) Meléndez & Barbuy (2009); (14) Kurucz (2013); (15) Smith (1988); (16) Smith & O'Neill (1975); (17) Aldenius et al. (2009); (18) Smith & Raggett (1981); (19) Smith (1981); (20) Wiese et al. (1966); (21) Storey & Zeippen (2000); (22) Froese Fischer & Tachiev (2012); (23) Ralchenko et al. (2010); (24) Pehlivan Rhodin et al. (2017); (25) Lawler et al. (2013); (26) Lawler et al. (2013).

Table A.3. Determined stellar parameters and abundances for observed giants.

HIP/KIC/TYC	$T_{\rm eff,ref}$	$T_{\rm eff}$	$\log g_{\rm ref}$	$\log g$	[Fe/H]	$v_{\rm mic}$	A(O)	A(Mg)	A(Ca)	A(Ti)
HIP 1692	...	4216	...	1.79	–0.29	1.55	...	7.50	6.10	4.68
HIP 9884	4493 ± 55	4464	...	2.27	–0.24	1.34	8.57	7.47	6.16	4.72
HIP 10085	...	4062	...	1.44	–0.35	1.63	...	7.37	6.03	4.60
HIP 12247	...	4790	...	2.71	–0.07	1.40	8.69	7.53	6.33	4.83
HIP 28417	...	4746	...	2.56	–0.28	1.40	8.63	7.44	6.16	4.67
HIP 33827	...	4235	...	1.99	–0.02	1.50	...	7.65	6.34	4.87
HIP 35759	...	4606	...	2.47	–0.18	1.42	8.74	7.63	6.25	4.80
HIP 37447	...	4758	...	2.73	–0.07	1.35	8.68	7.55	6.28	4.78
HIP 37826	4858 ± 60	4835	...	2.93	0.04	1.24	8.69	7.63	6.43	4.92
HIP 43813	...	4873	...	2.62	–0.10	1.51	8.66	7.49	6.33	4.77

Notes. Reference values for $T_{\rm eff}$ are from Mozurkewich et al. (2003) and the reference values for $\log g$ are from Huber et al. (2014). This is only an excerpt of the table to show its form and content. The complete table is available in electronic form at the CDS.